Potential Vorticity Diagnosis of the Factors Affecting the Movement of Typhoon Sinlaku (2002)

Chun-Chieh Wu, Treng-Shi Huang, and Kun-Hsuan Chou
Department of Atmospheric Sciences, National Taiwan University

Tien-Chiang Yeh
Central Weather Bureau

Abstract

Potential vorticity diagnostics is applied to study the factors affecting the slow-down processes of the movement of Typhoon Sinlaku (2002) as it approached the offshore of northeastern Taiwan. The analysis indicates that the initial deceleration was mainly associated with the retreat of the Pacific Subtropical High (SH) and the influence of the deepening mid-latitude trough (TR). The upper-level cold core low (CCL) played a minor role in impeding Sinlaku from moving northward, while the continental high (CH) over Mainland China kept steering Sinlaku westward. As the steering effect from the above four systems (SH, TR, CCL, and CH) tended to offset each other, the subtle interaction among them makes a precise track forecast difficult. The follow-up analysis on why and how the models fail to predict the slow-down of Sinlaku should have important implications on the future observing and modeling strategies to improve the forecasts of such type of typhoons.

1. Introduction

Typhoon Sinlaku (2002) formed over the north Western Pacific on 29 August, 2002 (Fig. 1), moved north-northwestward in the incipient two days, and then moved due west-northwestward following the steering flow associated with the Pacific High. By 0000 UTC 31 August, it had intensified into a moderate-strength typhoon, moving west northwestward at a speed of 7 m s^{-1} along the southern edge of the Pacific Subtropical High (SH) and remaining at the same course for the next four days. After Sinlaku passed through the longitude of 130° E at 1200 UTC 4 September, its translation speed started to slow down, decelerating from 5.5 m s^{-1} to 3.5 m s^{-1} at 0000 UTC 5 September. The speed further decreased to 2 m s^{-1} at 1200 UTC 5 September and on 6^{th}, during which period Sinlaku exhibited a west southwestward, then west northwestward track. It accelerated after 1800 UTC 6 September, made landfall in Fukien of Mainland China at 7^{th} 1200 UTC, and finally weakened into a tropical perturbation.

Typhoon Sinlaku was initially steered by the Pacific Subtropical High (SH); during its decelerating period from 1200 UTC 4 September to 5^{th} 1200 UTC, when the coverage of the 5880-gmp-contour at 500 hPa retreated from the central China to the east of 130°E (Figs. 2a, b). At 1200 UTC 5 September (Fig. 2c) Sinlaku was located at 125.8°E, 26.5°N, with an upper-level cold-core low (CCL) present near 139°E, 27°N, the SH to the east of the CCL, a mid-latitude trough (TR) over Korea, and a continental high (CH) over central China (see Fig. 2c).

The steering flow became quite weak between 0000 to 1200 UTC 6 September, due to the complicated configuration of the flow patterns associated with the SH, CCL, CH, and TR (Figs. 2d, e), thus making it difficult to accurately estimate the steering flow, not to mention the prediction of the storm motion. Indeed, at 1800 UTC 3 September, all official forecasts from the Central Weather Bureau of Taiwan, Japan Meteorological Agency, and Joint Typhoon Warning Center predicted that Sinlaku would make landfall at northeastern Taiwan 72h later (i.e., 1800 UTC 6 September). However, Sinlaku did not make landfall at Taiwan as predicted. It moved slightly southward for only about 0.4° between 1200 UTC 5 September and 0000 UTC 6 September before heading west northwestward for the southern Mainland China. Such a subtle error in track prediction resulted in a huge error in wind and rainfall prediction in the northern Taiwan, and led to rather great societal consternation due to the over warning of the storm.

In this paper the potential vorticity (PV) diagnosis (Wu and Emanuel 1995; Shapiro 1996; Wu et al. 2000) is employed to address the following questions: 1) Why Sinlaku slowed down; 2) What are the key factors affecting such slow-down processes; and 3) Why the operational numerical models failed to predict such processes, and how we can improve them. By evaluating the relative contribution to the steering flow from the aforementioned individual dynamical system, such as the SH, CCL, TR, and CH, through the so-called piecewise PV inversion, we can better understand why and how Sinlaku changed its path. Answers to the above questions can also provide useful information to

Corresponding author address: Chun-Chieh, Wu, Dept. of Atmospheric Sciences, National Taiwan University, 61, Ln. 144, Sec. 4, Keelung Rd., Taipei 10772, Taiwan. E-mail: cwu@typhoon.as.ntu.edu.tw

help form new observing and modeling strategies to improve the forecasts of such type of typhoons.

2. Methodology

2.1 Concept of the PV inversion

The use of PV for understanding the evolution of the dynamical system in the atmosphere has been well reviewed in Hoskins et al. (1985). Such a merit is particularly enhanced with its inversion characteristics. The PV inversion states that given a distribution of PV, a prescribed balanced condition, and boundary conditions, the balanced mass and wind fields can be recovered. Using the nonlinear balanced condition (Charney 1955) to invert the Ertel PV, Davis and Emanuel (1991) and Wu and Emanuel (1995) were able to quantitatively examine extratropical cyclogenesis and the steering of tropical cyclones, individually. Formulated on the π [$\pi = C_P(p/p_0)^{\kappa}$] coordinate and spherical coordinates, the two equations to be solved are:

$$q=\frac{g\kappa\pi}{p}\left[(f+\nabla^2\Psi)\frac{\partial^2\Phi}{\partial\pi^2}-\frac{1}{a^2\cos^2\phi}\frac{\partial^2\Psi}{\partial\lambda\partial\pi}\frac{\partial^2\Phi}{\partial\lambda\partial\pi}-\frac{1}{a^2}\frac{\partial^2\Psi}{\partial\phi\partial\pi}\frac{\partial^2\Phi}{\partial\phi\partial\pi}\right],$$

and

$$\nabla^2\Phi=\nabla\cdot(f\nabla\Psi)+\frac{2}{a^4\cos^2\phi}\frac{\partial(\partial\Psi/\partial\lambda,\partial\Psi/\partial\phi)}{\partial(\lambda,\phi)}.$$

where q represents PV, Φ represents geopotential height, Ψ represents stream function, "a" is the earth's radius, f is the Coriolis parameter,, $\kappa=R_d/C_p$, ψ longitude, and λ latitude. Given the distribution of q, the lateral boundary of Φ and Ψ, and the θ on the upper and lower boundaries, the distribution of Φ and Ψ can be solved. Therefore, the non-divergent wind and potential temperature can also be obtained by the following two relations:

$$\vec{V}=\hat{k}\times\nabla\Psi, \text{ and } \theta=-\frac{\partial\phi}{\partial\pi}.$$

Another robust strength associated with the PV inversion is the so-called piecewise PV inversion, i.e., when the flow field is appropriately divided into the mean and perturbation components, the above equations can be re-derived (Davis 1992) to obtain the balanced fields associated with each individual PV perturbation. Such methods provide a succinct approach to understand how the dynamical systems (PV fields) interact with each other, and how the tropical cyclone track is affected by different PV features in the observational data (Wu and Emanuel 1995; Shapiro 1996, 1999), and in the modeling atmosphere (Wu and Kurihara 1996).

2.2 The Shapiro (1996) decomposition

Shapiro (1996) devised a decomposition by taking the axisymmetric vortex as the mean field and the rest as the perturbation, and successfully showed that such decomposition can clearly demonstrate how the environmental perturbation interacts with the tropical cyclone vortex.

In this research, to understand how Sinlaku was steered by the perturbation flow field (such as those associated with the SH, TR, CCL, and CH), we take the axisymmetric average relative to the center of Sinlaku as the mean part, and then follow the approach of Shapiro (1996) to perform the piecewise PV inversion. In other words, we first construct the azimuthal average of the wind field to obtain the average stream function $\overline{\Psi}$, so that the associated average geopotential height can be derived from the nonlinear balanced equation,

$$\nabla^2\hat{\Phi}=\nabla\cdot(f_0\nabla\overline{\Psi})+\frac{2}{a^4\cos^2\phi}\frac{\partial(\partial\overline{\Psi}/\partial\lambda,\partial\overline{\Psi}/\partial\phi)}{\partial(\lambda,\phi)}.$$

The averaged PV field is then calculated by the following relation,

$$\hat{q}=\frac{g\kappa\pi}{p}\left[(f+\nabla^2\overline{\Psi})\frac{\partial^2\hat{\Phi}}{\partial\pi^2}-\frac{1}{a^2\cos^2\phi}\frac{\partial^2\overline{\Psi}}{\partial\lambda\partial\pi}\frac{\partial^2\hat{\Phi}}{\partial\lambda\partial\pi}-\frac{1}{a^2}\frac{\partial^2\overline{\Psi}}{\partial\phi\partial\pi}\frac{\partial^2\hat{\Phi}}{\partial\phi\partial\pi}\right]$$

By taking the perturbation field as $\psi'=\psi-\overline{\psi}$, $\phi'=\phi-\hat{\phi}$, and $q'=q-\hat{q}$, the piecewise PV inversion can be performed to calculate the balanced flow and mass fields associated with each PV perturbation. In this study, to show how the flow field attributed to different dynamical systems affected the motion of Sinlaku, the whole PV perturbation (Q') is divided into several parts, e.g., $Q'(SH)$, $Q'(CH)$, $Q'(TR)$, and $Q'(CCL)$, which represents the PV perturbation associated with SH, CH, TR, CCL, individually. Meanwhile, $Q'(OT)$ indicates the whole PV perturbation other than the above four perturbations. Note that by definition, $Q'=Q'(SH)+Q'(CH)+Q'(TR)+Q'(CCL)+Q'(OT)$

2.3 Data

The NCEP-AVN (National Centers for Environmental Prediction - Aviation model) global analysis is used for the above PV diagnosis. The AVN analysis has a resolution of 1° × 1°, 181 (meridional direction) × 360 (zonal direction) grids, and 26 vertical pressure levels.

3. Results

Following Wu et al. (2000), to evaluate the steering flow due to various PV perturbations, the deep-layer (975 – 300 hPa) mean wind averaged over the inner 3° of the storm center is used throughout the paper, and is demonstrated in both Figs. 3 and 4. In general the deep-layer steering flow from the AVN analysis is very close to the actual best track in the whole time period of this study. The error is always less than about 1 m s^{-1} (cf. the bottom two wind barbs in Fig. 3), indicating that it is valid to use the PV inversion to diagnose the steering flow associated with each individual PV perturbation. To highlight the issues on the factors affecting the slow-down processes of Sinlaku, only the time period between 1200 UTC 4 September and 0000 UTC 7 September is investigated here. Special emphasis is also put on the relative role of the SH, CCL, CH, and TR on the steering of Sinlaku based on the piecewise PV inversion.

It is found in Figs. 3 and 4 that the presence of CCL contributed a 1.5 m s^{-1} southward advection of Sinlaku during 1200 UTC 4 September to 0000 UTC 6 September. As the CCL moved further east by the TR after 0600 UTC 6 September, it was farther away from Sinlaku and had less southward steering effect over Sinlaku. This result may also help explain why Sinlaku moved slightly toward the north after 1200 UTC 6 September (Fig. 3).

During the time period from September 4 to September 6, the translation speed of Sinlaku kept decreasing, which is consistent with the reduction of the steering flow [associated with the weakening Q' (SH)] from 8 m s^{-1} at 1200 UTC 4 September, to 5 m s^{-1} at 1800 UTC 6 September (Fig. 3). Meanwhile, as the SH retreated, the separation of the SH and Sinlaku by the presence of the CCL is another factor limiting the influence of the SH on the motion of Sinlaku.

On the other hand, the steering flow associated with Q' (CH) constantly advected Sinlaku southwestward at about 7 ~ 8 m s^{-1}. The summation of the steering flow associated with Q'(SH) and Q'(CH) provided a west southwestward motion, which is much larger than the actual motion of Sinlaku. Apparently there must be some missing eastward advection effect from other dynamical systems. Indeed, it is the Q'(TR) that provided a strong eastward steering flow, peaking at 8 m s^{-1} at 0600 UTC 6 September. The result here strongly suggests that the strengthening of the eastward steering due to the deepening TR plays a crucial role on the deceleration of Sinlaku.

Interestingly, the steering flow associated with Q'(SH), Q'(CH) and Q'(TR) (see Fig. 3) is fairly close to the actual motion of Sinlaku, indicating their dominant role in affecting the movement of Sinlaku. In all, during the period from 1200 UTC 4 September to 5 September, the slow-down of Sinlaku is mainly related to the weakening of the SH and the approaching TR. After 0600 UTC 6 September, as the influence from TR gradually decreased, such an effect on steering flow tended to be off-balanced by the continuous weakening of SH. Therefore the impact from CH gradually dominated, and led to the acceleration of Sinlaku toward Mainland China on September 7.

4. Summary

Typhoons over the North western Pacific often move westward or northwestward due to the dominating steering flow associated with the Pacific Subtropical High (SH). However during the late season in some cases as the typhoons approached about 130°E, due to the weaking of the SH, as well as the strengthening of the Continental High (CH) over Mainland China and/or the presence of the deep mid-latitude baroclinic wave/trough (TR), typhoons may slow down or even stall. Sinlaku is a case in point to indicate such scenario, while most of the operational forecasting model failed to predict its slow-down process.

In this study the potential vorticity diagnostics is applied to investigate the factors affecting the slow-down process of the movement of Typhoon Sinlaku as it approached the offshore of northeastern Taiwan. The analysis indicates that the initial deceleration was mainly associated with the retreat of the Pacific Subtropical Height (SH) and the influence of the deepening mid-latitude trough (TR). The upper-level cold core low (CCL) played a minor role in impeding Sinlaku from moving northward, while the continental high (CH) over Mainland China kept steering Sinlaku westward. As the steering effect from the above four systems (SH, TR, CCL, and CH) tends to offset each other, the subtle interaction among them makes it difficult to have a precise track forecast.

The relative steering effect from the SH, TR, CCL, and CH appeared to play a crucial role on typhoon tracks in this area. Work is undertaken to study why and how the numerical models failed to predict the slow-down processes based on the PV diagnosis of the model outputs. The results should have important implication on the future observing (Aberson 2002) and modeling strategies to improve the forecasts of such type of typhoons.

References

Aberson, S. D., 2002: Targeted observations to improve operational tropical cyclone track forecast guidance. Submitted to Mon. Wea. Rev.

Charney, J. G., 1955: The use of primitive equations of motion in numerical prediction. Tellus, 7, 22-26.

Davis, C. A., , and K. A. Emanuel, 1991: Potential vorticity diagnostics of cyclogenesis. Mon. Wea. Rev., 119, 1925-1953.

——, 1992a: A potential-vorticity diagnosis of the importance of initial structure and condensational heating in observed extratropical cyclogenesis. Mon.Wea. Rev., 120, 2409-2428.

Hoskins, B. J., M. E. McIntyre, and A. W. Robertson, 1985: On the use and significance of isentropic potential-vorticity maps. Quart. J. Roy. Meteor. Soc., 111, 877-946.

Shapiro, L. J. , 1996: The motion of Hurricane Gloria: A potential vorticity diagnosis. Mon. Wea. Rev., 124, 1497-2508.

——, 1999: Potential vorticity asymmetries and tropical cyclone motion. Mon. Wea. Rev., 127, 124-131.

Wu, C.-C., and K. A. Emanuel, 1995: Potential vorticity diagnostics of hurricane movement. Part I: A case study of Hurricane Bob (1991). Mon. Wea. Rev., 123, 69-92.

____, and Y. Kurihara, 1996: A Numerical Study of the Feedback Mechanisms of Hurricane-Environment Interaction on Hurricane Movement from the Potential Vorticity Perspective. J. Atmos. Sci., 53, 2264-2282.

——, T.-S. Huang, K.-N. Huang, and T.-C. Yeh, 2000: PV Diagnostics of the Impact of Model Initialization on the Performance of a Typhoon Prediction System. Proc. 24th Conf. on Hurricanes and Tropical Meteorology. American Meteorological Society, Boston MA, 423-424.

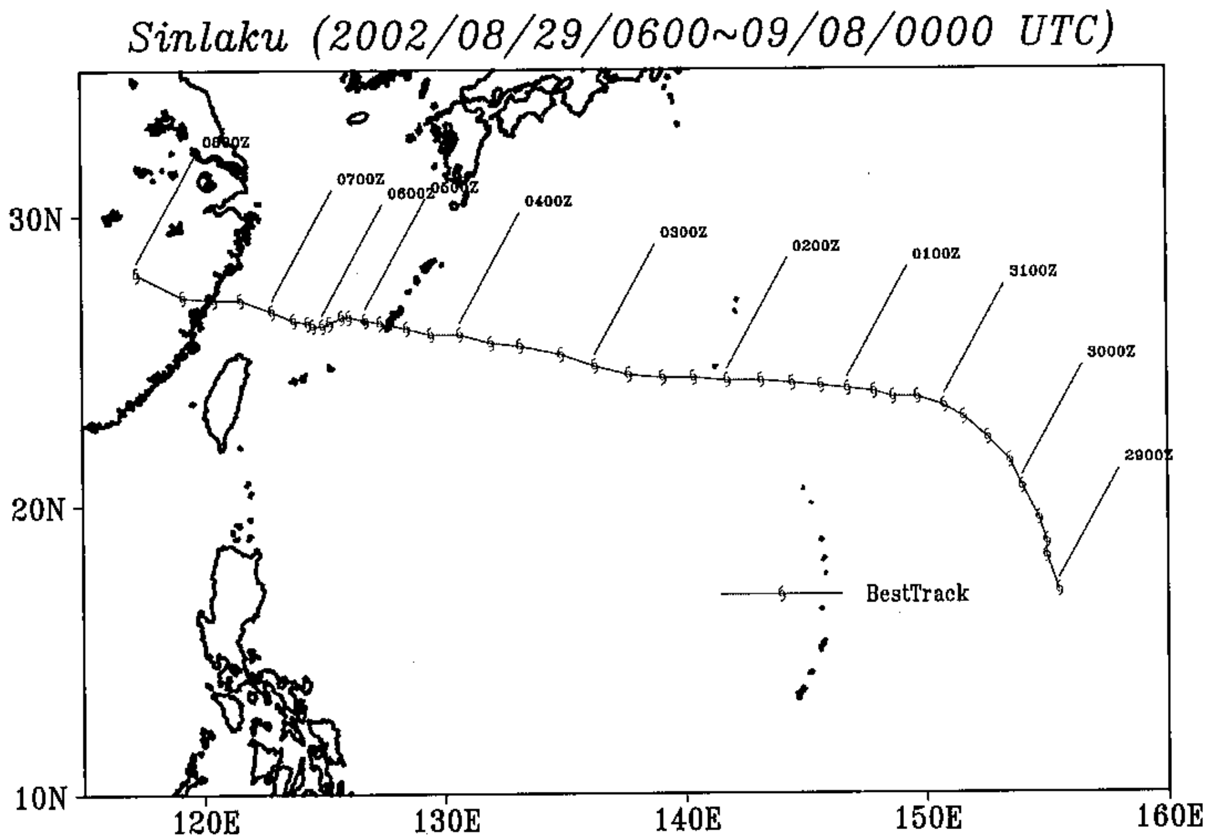

Fig. 1 Best tracks (CWB) of Typhoon Sinlaku (2002) (indicated by the typhoon symbol for every 6h) from 0600 UTC Augst 29 to 0000 UTC 8 September, 2002.

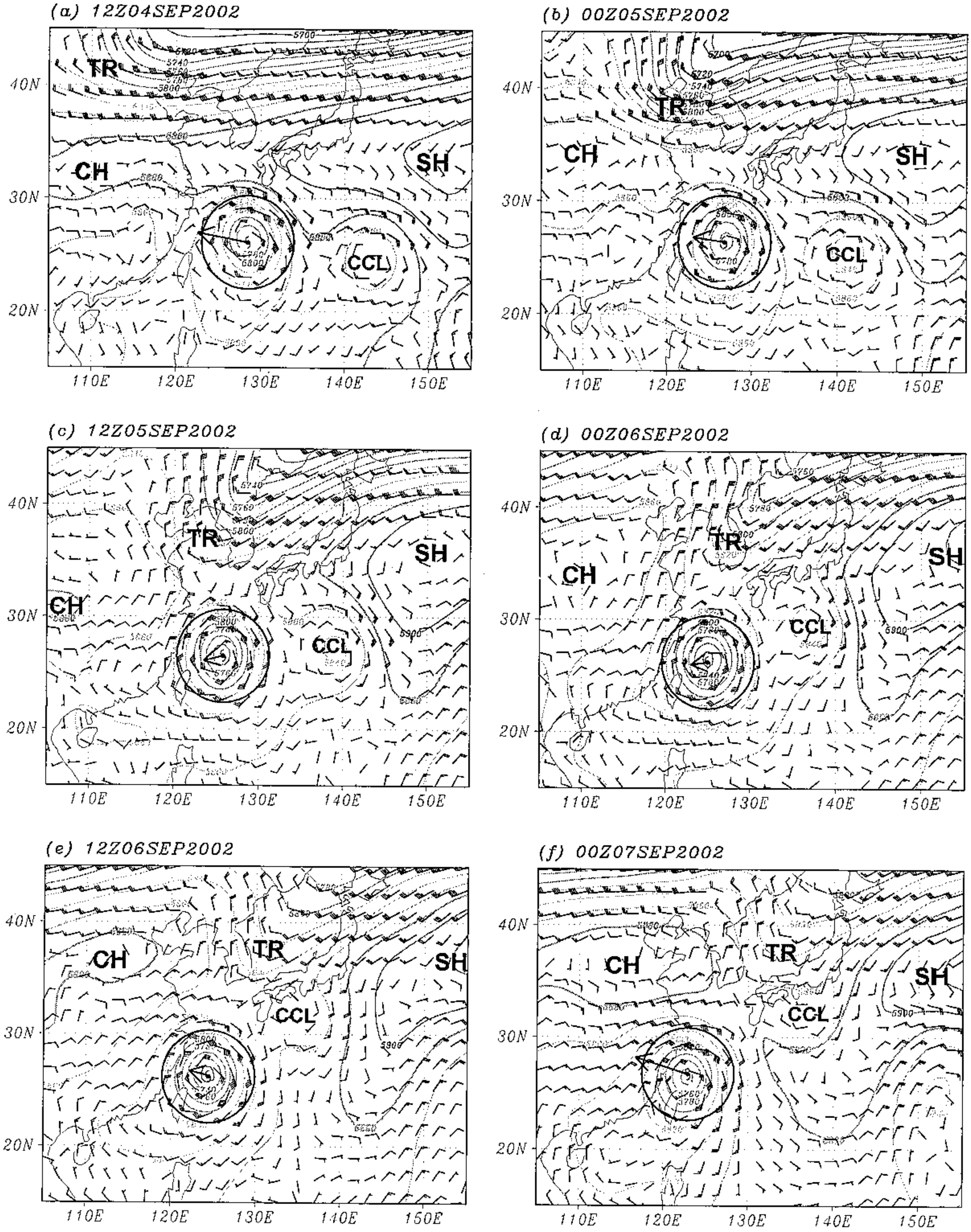

Fig. 2 500-mb geopotential height (with contour interval of 20 m) and wind (Full barb= 5 m s^{-1}) starting form 1200 UTC Sep. 04, to 0000 UTC Sep. 07 2002. The instantaneous movement of Sinlaku is indicated by an arrow, whose length represents the actual translation velocity, and the circle shows the scale of 5 m s^{-1}.

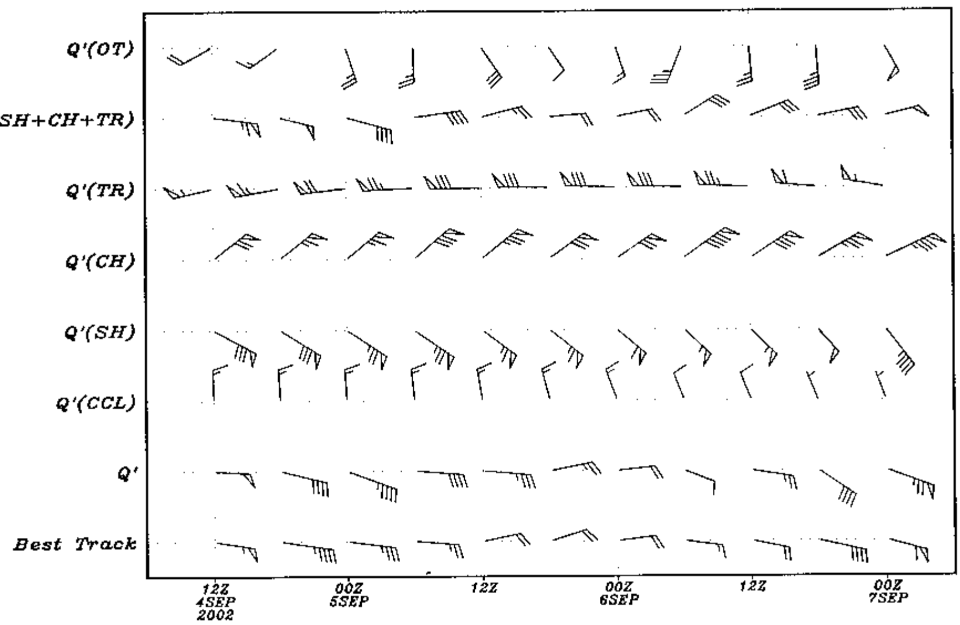

Fig. 3 The movement of Sinlaku and the steering flow (averaged in the inner 3 latitude degree between 975 and 300 hPa) associated with the total PV perturbation, $Q'(SH)$, $Q'(CH)$, $Q'(TR)$, $Q'(CCL)$, and $Q'(OT)$. $Q'(SH)$, $Q'(CH)$, $Q'(TR)$, and $Q'(CCL)$ represents the PV perturbation associated with SH, CH, TR, and CCL, individually, while $Q'(OT)$ represents the PV perturbation other than the above four perturbations. One full wind barb represents 1 m s^{-1}.

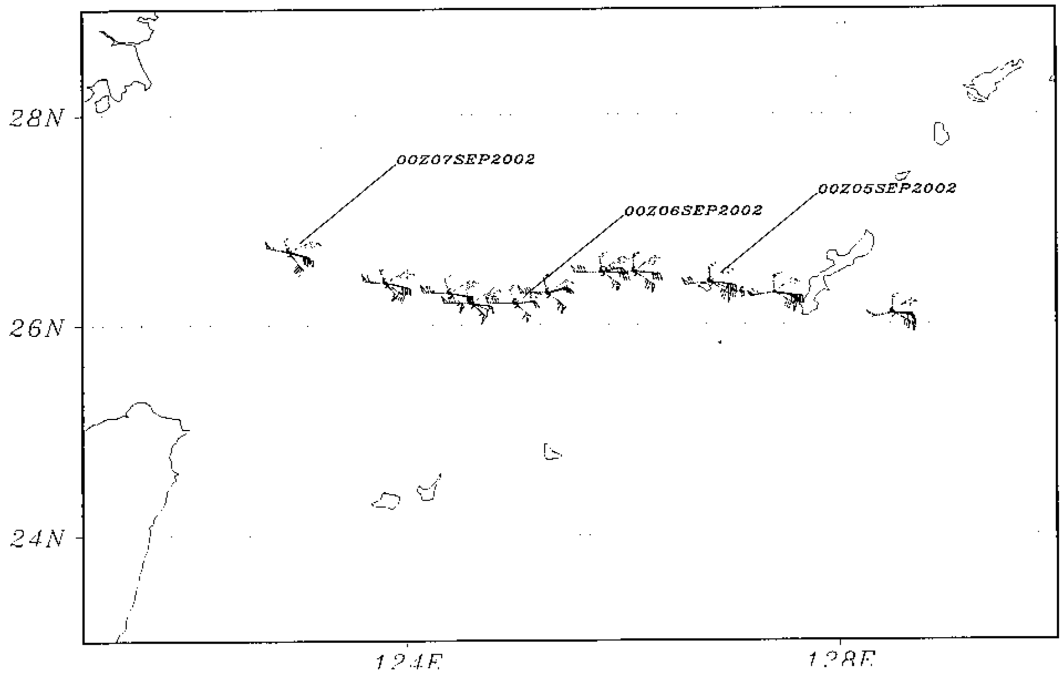

Fig. 4 The movement of Sinlaku (black) and the steering flow (averaged in the inner 3 latitude degree between 975 and 300 hPa) associates with the total PV perturbation (red), $Q'(SH)$ (dark blue), $Q'(CH)$(blue), $Q'(TR)$ (pink), and $Q'(CCL)$ (green). $Q'(SH)$, $Q'(CH)$, $Q'(TR)$, and $Q'(CCL)$ represent the PV perturbation associated with SH, CH, TR, and CCL, individually. One full wind barb represents 1 m s^{-1}.